

THE SOURCES OF THE COSMIC INFRARED BACKGROUND

Guilaine Lagache, Hervé Dole, Jean-Loup Puget

Institut d'Astrophysique Spatiale (IAS), Bâtiment 121, F-91405 Orsay (France); Université Paris-Sud 11 and CNRS (UMR 8617)

Abstract. The discovery of the Cosmic Infrared Background (CIB) in 1996, together with recent cosmological surveys from the mid-infrared to the millimeter have revolutionized our view of star formation at high redshifts. It has become clear, in the last decade, that a population of galaxies that radiate most of their power in the far-infrared (the so-called “infrared galaxies”) contributes an important part of the whole galaxy build-up in the Universe. Since 1996, detailed (and often painful) investigations of the high-redshift infrared galaxies have resulted in the spectacular progress reviewed in this paper. Among others, we emphasize a new *Spitzer* result based on a Far-IR stacking analysis of mid-IR sources.

1 Introduction

The CIB can be defined as the part of the present radiation content of the Universe made essentially of the long-wavelength output from all sources throughout the history of the Universe. Fig. 1 shows the cosmic background due to sources from the UV up to the mm. It has two maxima, one in the optical and one in the far-IR with roughly equal brightness and with a minimum at 5 microns. This minimum is created by the decrease of brightness of the stellar component with λ combined with the rising brightness of the dust. The CIB is defined as the cosmic background at λ longward of this minimum. An understanding of the nature and redshift distribution of the sources of the CIB, although relatively new, is an integral part of our understanding of the formation and evolution of galaxies.

The *IRAS* satellite, launched in 1983 gave for the first time a proper census of the infrared emission of galaxies at low redshift. The Luminosity Function (LF) at 60 and 100 μm is dominated by L_* spiral galaxies as could be expected – the reradiated stellar luminosity absorbed by dust. In addition, a high-luminosity tail of luminous galaxies was found (e.g. Sanders & Mirabel 1996). This high-luminosity tail can be approximated by a power-law, $\Phi(L) \propto L_{\text{IR}}^{2.35}$, which gives a space density for the most luminous infrared sources well in excess of predictions based on the optical LF. These sources comprise the Luminous Infrared Galaxies, LIRGs, and the ULIRGs with luminosities $11 < \log(L_{\text{IR}}/L_{\odot}) < 12$ and $\log(L_{\text{IR}}/L_{\odot}) > 12$, respectively. These galaxies are often associated with interacting or merging, gas-rich disks. They do not dominate the energy production locally. As an example, the total infrared luminosity from these galaxies in the *IRAS* Bright Galaxy Sample accounts for only $\sim 6\%$ of the infrared emission in the local Universe (Soifer & Neugebauer, 1991). The situation changes dramatically at higher redshift where these galaxies fully dominate the infrared energy output. We just give here for illustration a very simple argument. We know that locally, the infrared output of galaxies is only one third of the optical output. In contrast, we observe in the cosmic background a power in the infrared comparable to the power in the optical. This implies that infrared galaxies grow more luminous with increasing z faster than do optical galaxies.

In addition to the CIB, the observations relevant to the problem of star and galaxy formation at high z from the mid-IR ($\sim 10 \mu\text{m}$) to the mm are the following:

- Deep number counts obtained at 15, 24, 90, 160, 170, 350/450, 850, 1200 μm (e.g. Dole et al. 2001, Elbaz et al. 2002, Scott et al. 2002, Dole et al. 2004, Greve et al. 2004, Héraudeau et al. 2004, Papovich et al. 2004,).
- Luminosity function up to $z \sim 1$ (e.g. Le Floch et al. 2005, Pérez-González et al. 2005)
- Clustering properties (e.g. Blain et al. 2004 for a first attempt at 850 μm)
- Power spectra of the unresolved background (Lagache & Puget 2000, Matsuhara et al. 2000, Miville-Deschênes et al. 2002, Maloney et al. 2005)
- Identifications and multi-wavelength observations of IR galaxies

We outline here the main results in this field. More details are given in Lagache et al. (2005).

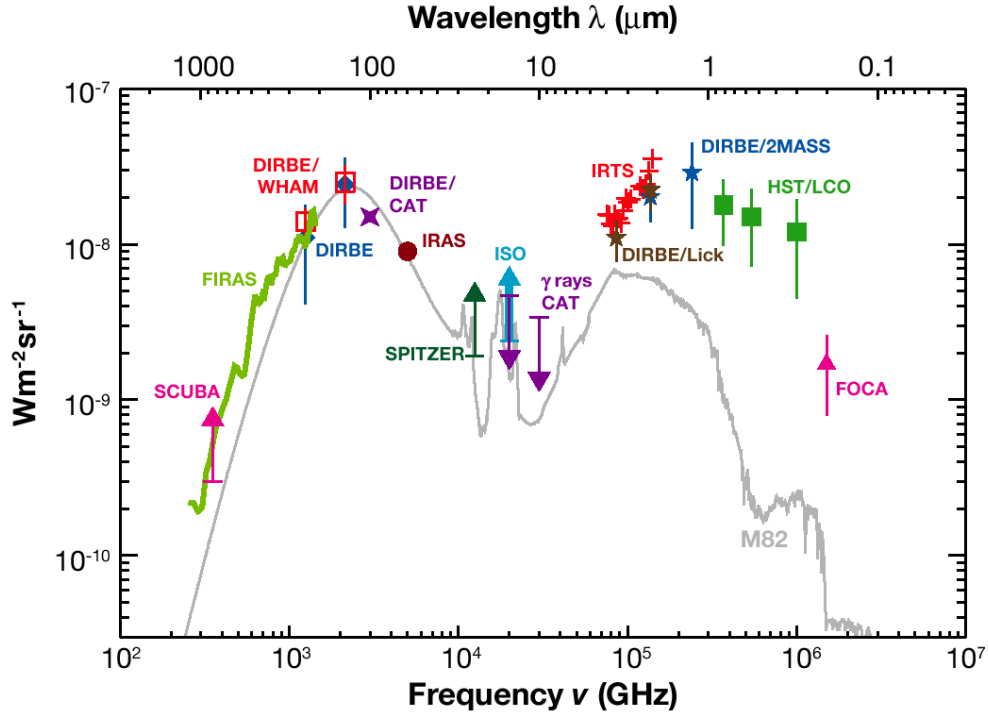


Figure 1: The extragalactic background over three decades in frequency from the near UV to millimeter wavelengths. Only strongly constraining measurements have been reported. We show for comparison in grey an SED of M82 (Chanial, 2003)– a starburst galaxy at $L=3 \times 10^{10} L_{\odot}$ – normalised to the peak of the CIB at $140 \mu m$. References for data points are given in Lagache et al. (2005).

2 Redshift distribution of the sources of the CIB

An other important property to note from the observation of the CIB is that the slope of the long wavelength part of the CIB, $I_{\nu} \propto \nu^{1.4}$ (Gispert et al. 2000), is much less steep than the long wavelengths spectrum of galaxies (as illustrated in Figure 1 with the M82 SED). This implies that the millimeter CIB is not due to the millimeter emission of the galaxies that account for the peak of the CIB ($\simeq 150 \mu m$). In fact, contributions from galaxies at various redshifts are needed to fill the CIB SED shape. The bulk of the CIB in energy, i.e., the peak at about $150 \mu m$, is not resolved in individual sources (as discussed in Sect. 3) but one dominant contribution at the CIB peak can be inferred from the ISOCAM deep surveys. ISOCAM galaxies with a median redshift of ~ 0.7 resolve about 80% of the CIB at $15 \mu m$. Elbaz et al. (2002) separate the $15 \mu m$ galaxies into different classes (ULIRGs, LIRGs, Starbursts, normal galaxies and AGNs) and extrapolate the $15 \mu m$ fluxes to $140 \mu m$ using template SEDs. A total brightness of $(16 \pm 5) \text{ nW m}^{-2} \text{ sr}^{-1}$ is found, which makes up about two thirds of the CIB observed at $140 \mu m$ by COBE/DIRBE. Hence, the galaxies detected by ISOCAM are responsible for a large fraction of energy of the CIB. However, these galaxies make little contribution to the CIB in the millimeter and submillimeter. There, the CIB must be dominated by galaxies at rather high redshift for which the SED peak has been shifted. The redshift contribution to the CIB is illustrated in Figure 2. We clearly see that the submillimeter/millimeter CIB contains information on the total energy output by the high-redshift galaxies ($z > 2$). This is supported by the redshift distribution of the SCUBA sources at $850 \mu m$ with $S_{850} \geq 3 \text{ mJy}$ that make about 30% of the CIB and have a median redshift of 2.2 (Chapman et al. 2005).

3 The Status of Deep Surveys: Resolved Fraction of the $>10 \mu m$ CIB

Many surveys from the mid-infrared to the millimeter have aimed to resolve the CIB into discrete sources (Table 1). From Table 1, we see that the most constraining surveys in term of resolving the CIB are those at 15 , 24 and $850 \mu m$. Moreover, the capabilities of these surveys to find high- z objects are the best among all other existing surveys (see Lagache et al. 2005). These surveys probe the CIB in well-defined and distinct redshift ranges,

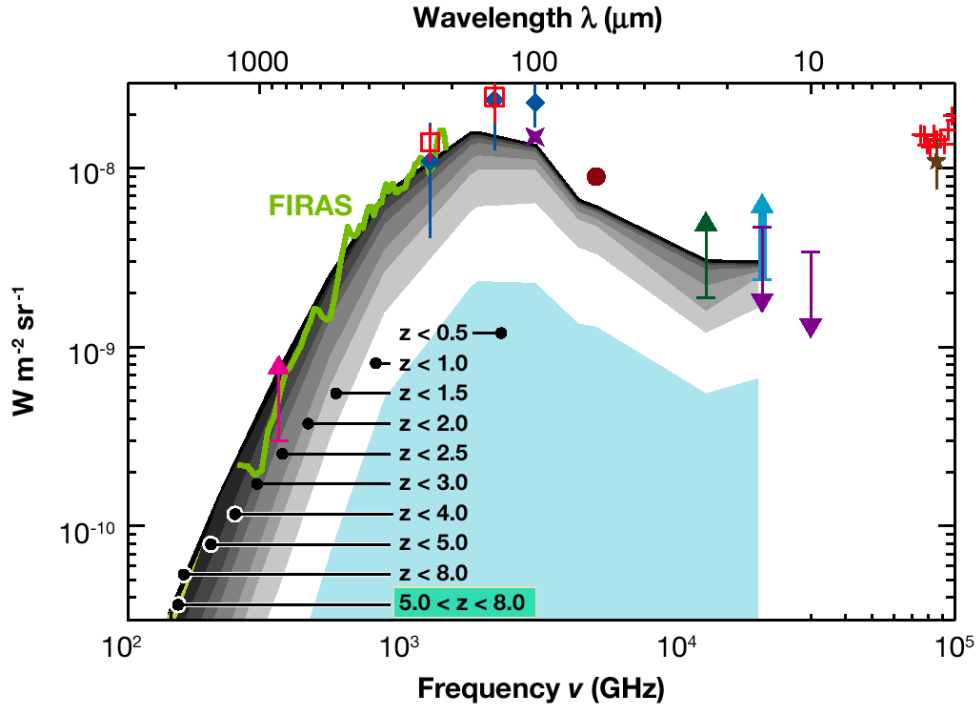


Figure 2: Cumulative contribution to the CIB of galaxies at various redshifts from 0.5 to 8, from the model of Lagache et al. (2004). Measurements of the CIB are reported with the same symbols as in Figure 1.

with median redshifts of 0.7 (Liang et al. 2004), ~ 1 (Caputi et al. 2005 and L. Yan, private communication), and 2.2 (Chapman et al. 2005) at 15, 24 and 850 μm , respectively. Such well-defined redshift ranges are due to the peculiar shape of K-corrections at these wavelengths.

4 Detailed properties of the sources of the CIB

4.1 The $0.5 < z < 1.5$ galaxies

At the time of writing, most of the detailed informations on dusty galaxies in the $0.5 \leq z \leq 1.5$ redshift range comes from galaxies selected with the ISOCAM cosmological surveys at 15 μm and the multi-wavelength analysis of detected sources. Shallow, deep and ultra-deep surveys were performed in various fields including the Lockman hole, Marano, northern and southern Hubble Deep Field (HDF), and Canada-France Redshift Survey (CFRS) (e.g., Aussel et al. 1999; Flores et al. 1999; Lari et al. 2001; Gruppioni et al. 2002; Mann et al. 2002; Elbaz & Cesarsky 2003; Sato et al. 2003). Deeper images have been made in the direction of distant clusters (e.g., Metcalfe et al. 2003). Finally, the bright end of the luminosity function was explored by the ELAIS survey (e.g., Oliver et al. 2000). The deepest surveys reach a completeness limit of about 100 μJy at 15 μm (without lensing). The most relevant data to this section are the deep and ultra-deep surveys.

To find out the nature and redshift distribution of the 15 μm deep survey sources, many followup observations have been conducted including HST imaging and VLT spectroscopy. With a point-spread function full width at half of maximum of 4.6 arcsec at 15 μm , optical counterparts are easily identified. Redshifts are found using emission and/or absorption lines. From field to field, the median redshift varies from 0.52 to 0.8, a quite large variation due to sample variance. Most of ISOCAM galaxies have redshifts between ~ 0.3 and 1.2, consistent with Figure 2. About 85% of the ISO galaxies show obvious strong emission lines (e.g., [OII] 3723, H_γ , H_β , [OIII] 4959, 5007). These lines can be used as a diagnostic of the source of ionization and to distinguish the HII-region like objects from the Seyferts and LINERs. Most of the objects are found to be consistent with HII regions, e.g., from Liang et al. (2004) and exhibit low ionization level ($[\text{OIII}]/\text{H}_\beta < 3$). From emission lines studies, the AGN fraction is quite low, $\sim 20\%$. This is consistent with X-ray observations of ISOCAM sources

Survey	Fraction of resolved CIB	Reference
ISOCAM 15 μ m	80%	Elbaz et al. 2002
SPITZER 24 μ m	70%	Papovich et al. 2004
SPITZER 70 μ m	23%	Dole et al. 2004
ISOPHOT 90 μ m	<5%	Héraudeau et al. 2004
SPITZER 160 μ m	7%	Dole et al. 2004
ISOPHOT 170 μ m	<5%	Dole et al. 2001
SCUBA 450 μ m	15%	Smail et al. 2002
SCUBA 850 μ m	60% (S>1 mJy)	Smail et al. 2002
	30% (S>3 mJy)	Lagache et al. 2005
MAMBO 1.2 mm	10%	Greve et al. 2004

Table 1: CIB resolved fraction

showing that AGNs contribute at most $17\pm 6\%$ of the total mid-infrared flux (Fadda et al. 2002). Assuming template SEDs typical of star-forming and starburst galaxies, 15 μ m fluxes can be converted into total infrared luminosities, L_{IR} (between 8 and 1000 μ m). About 75% of the galaxies dominated by the star formation are either LIRGs or ULIRGs. The remaining 25% are nearly equally distributed among either "starbursts" ($10^{10} < L_{\text{IR}} < 10^{11} L_{\odot}$) or "normal" ($L_{\text{IR}} < 10^{10} L_{\odot}$) galaxies. The median luminosity is about $3 \times 10^{11} L_{\odot}$. ULIRGs and LIRGs contribute to about 17% and 44% to the CIB at 15 μ m, respectively (Elbaz et al. 2002). This suggests that the star formation density at $z < 1$ is dominated by the abundant population of LIRGs (see also Le Floch et al. 2005). Because of large extinction in LIRGs and ULIRGs, the infrared data provide more robust SFR estimate than UV tracers. The extinction factor in LIRGs averages to $A_V \sim 2.8$ at $z \sim 0.7$ (Flores et al. 2004). It is much higher than that of the local star-forming galaxies for which the median is 0.86 (Kennicutt 1992). Assuming continuous burst of age 10-100 Myr, solar abundance, and a Salpeter initial mass function, the SFR can be derived from the infrared luminosities (Kennicutt 1998). Typical LIRGs form stars at $\geq 20 M_{\odot} \text{ year}^{-1}$. The median SFR for the 15 μ m galaxies is about $50 M_{\odot} \text{ year}^{-1}$, a substantial factor larger than that found for faint-optimally selected galaxies in the same redshift range.

The other fundamental parameter characterizing the sources of the peak of the infrared background is their stellar mass content that traces the integral of the past star formation activity in the galaxies and is a natural complement to the instantaneous rate of star formation. The stellar masses can be obtained using spectral synthesis code modeling of the UV-optical-near infrared data or, more simply using the mass-to-luminosity ratio in the K-band. The derived stellar masses for the bulk of ISOCAM galaxies range from about 10^{10} to $3 \times 10^{11} M_{\odot}$, compared to $1.8 \times 10^{11} M_{\odot}$ for the Milky Way. As expected from the selection based on the LW3 flux limit – and thus on the SFR – masses do not show significant correlation with redshift (Franceschini et al. 2003). An estimate of the time spent in the starburst state can be obtained by comparing the rate of ongoing star formation (SFR) with the total mass of already formed stars: $t[\text{years}] = M/\text{SFR}$. Assuming a constant SFR, t is the timescale to double the stellar mass. For LIRGs at $z > 0.4$, t ranges from 0.1 to 1.1 Gy with a median of about 0.8 Gyr (Franceschini et al. 2003; Hammer et al. 2005). From $z = 1$ to $z = 0.4$ (i.e., 3.3 Gyr), this newly formed stellar mass in LIRGs corresponds to about 60% of the $z = 1$ total mass of intermediate mass galaxies. The LIRGs are shown to actively build up their metal content. In a detailed study, Liang et al. (2004) show that, on average, the metal abundance of LIRGs is less than half of the $z \sim 0$ disks with comparable brightness. Expressed differently, at a given metal abundance, all distant LIRGs show much larger B luminosities than local disks. Assuming that LIRGs eventually evolve into the local massive disk galaxies, Liang et al. (2004) suggest that LIRGs form nearly half of their metals and stars since $z \sim 1$.

Finally, morphological classification of distant LIRGs is essential to understand their formation and evolution. Zheng et al. (2004) performed a detailed analysis of morphology, photometry, and color distribution of 36 ($0.4 < z < 1.2$) ISOCAM galaxies using HST images. Thirty-six percents of LIRGs are classified as disk galaxies with Hubble type from Sab to Sd; 25% show concentrated light distributions and are classified as Luminous Compact Galaxies (LCGs); 22% display complex morphology and clumpy light distributions and are classified as irregular galaxies; only 17% are major ongoing mergers showing multiple components and apparent tidal tails. This is clearly different from the local optical sample of Nakamura et al. (2004) in the same mass range in which 27%, 70%, <2%, 3% and <2% are E/S0, spirals, LCGs, irregulars and major mergers respectively. For most compact LIRGs, the color maps reveal a central region strikingly bluer than the outer regions. These blue central regions have a similar size to that of bulges and a color comparable to that of star-forming regions. Because the bulge/central region in local spiral is relatively red, such a blue core structure could imply that the galaxy was forming the bulge (consistent with Hammer et al. 2001). It should be noticed that they find all LIRGs distributed along a sequence that relates their central color to their compactness. This is expected if star formation occurs first in the center (bulge) and gradually migrate to the outskirts (disk), leading to redder colors of the central regions as the disk stars were forming (see also Hammer et al., this conference).

4.2 The $z > 1.5$ galaxies

Analysis of the CIB in the light of the ISO observations shows that, as we go to wavelengths much longer than the emission peak, the CIB should be dominated by galaxies at higher redshifts. The main source of observations of the submm/mm CIB are the SCUBA submillimeter observations at $850 \mu\text{m}$ and $450 \mu\text{m}$ (see Blain et al 2002 for a review) and observations from the MAMBO instrument on the IRAM 30-m telescope at 1.2 mm (Greve et al. 2004). The first obvious question when investigating the nature of the submillimeter galaxies (SMGs) is thus their redshift distribution. The rather low angular resolution of the submillimeter and millimeter observations made identifications with distant optical galaxies an almost impossible task without an intermediate identification. This is provided by radio sources observed with the VLA with 10 times better angular resolution. The tight correlation between far-infrared luminosity and radio flux (Helou et al. 1985; Condon 1992) provides the needed link. This then allows us to get optical identifications and redshift measurements using 10-m class telescopes. Confirmation of these identifications can then be obtained through CO line observations with the millimeter interferometers such as the Plateau de Bure interferometer. The redshift deduced from the optical lines is confirmed by the CO observations. So far, only a handful of cases have gone through this whole chain of observations (e.g., Genzel et al. 2003; Greve et al. 2005; Neri et al. 2003), but a high success rate gives confidence in the first step of the identification process. Chapman et al. (2005) got spectroscopic redshifts of 73 sources obtained using the radio identification. The redshift distribution peaks at $z=2.2$ with a substantial tail up to $z=4$. Almost all SMGs are found in the redshift range $1.5 < z < 3$.

Many LIRGs and ULIRGs at low redshifts have been identified with interacting or galaxy mergers. A substantial fraction show signs of AGN activity but it has been shown for the low-redshift LIRGs and ULIRGs that the starburst component dominates the energy output (Genzel et al. 1998; Lutz et al. 1998). The sources used for the redshift distribution of Chapman et al. (2005) have been imaged with the HST. Most of them are multi-component-distorted galaxy systems (Conselice et al. 2003; Smail et al. 2004). They display irregular and frequently highly complex morphologies compared to optically selected galaxies at similar redshifts. They are often red galaxies with bluer companions, as expected for interacting, star-forming galaxies. They have higher concentrations, and more prevalent major-merger configurations than optically-selected galaxies at $z \sim 2-3$. Most strikingly, most of the SMGs are extraordinarily large and elongated relative to the field population regardless of optical magnitude. SMGs have large bolometric luminosities, $\sim 10^{12} - 10^{13} L_{\odot}$, characteristic of ULIRGs. If the far-infrared emission arises from the star formation, the large luminosities translate to very high SFR $\geq 1000 M_{\odot} \text{ year}^{-1}$. Such high rates are sufficient to form the stellar population of a massive elliptical galaxy in only a few dynamical times, given a sufficient gas reservoir. SMGs are very massive systems with typical mass of $1-2 \times 10^{11} L_{\odot}$ (Swinbank et al. 2004), comparable to the dynamical mass estimates from CO observations. Genzel et al. (2004; and more recently Greve et al. 2005) have undertaken an ambitious program to study the nature of the SMGs in more details. They got CO spectra with the Plateau de Bure interferometer for 7 sources out of their sample of 12 for the CO 3-2 and 4-3 transitions redshifted in the 3 mm atmospheric window. They provide optical identifications and redshifts. The detection of these sources at the proper redshift confirms the usefulness of identification with the help of the radio sources. The median redshift of this sample is 2.4. In addition, one source was studied with the SPIFI instrument on the ESO/VLT. These observations are giving very interesting clues on the nature of the submillimeter galaxies. The gas masses obtained for these systems using CO luminosity/mass of gas determined from local ULIRGs is very large with a median of $2.2 \times 10^{10} M_{\odot}$ (10 times larger than in the Milky Way). Using the velocity dispersion, they could infer that the dynamical median mass of these systems is 13 times larger than in Lyman-break galaxies (LBGs) at the same redshift or 5 times the mass of optically selected galaxies at this redshift. These SMGs with a flux at $850 \mu\text{m}$ larger than 5 mJy are not very rare and unusual objects, because they contribute to about 20% of the CIB at this frequency. Through multiwavelength observations, Genzel et al. (2004) get the stellar component in K band, and infer the star-formation rate and duration of the star-formation burst. They can then compare the number density of these massive systems with semiempirical models of galaxy formation. The very interesting result is that this number density is significantly larger than the predicted one, although the absolute numbers depends on a number of assumptions like the IMF. Such massive systems at high redshift are not easy to understand in current cold dark matter hierarchical merger cosmogonies. However, one must keep in mind that bright SMGs ($S_{850} > 5 \text{ mJy}$) that contribute 20% of the CIB may not be representative of the whole population. Gravitational lens magnification provides a rare opportunity to probe the nature of the distant sub-mJy SMGs. Kneib et al. (2005) study the property of one SMG with an $850 \mu\text{m}$ flux $S_{850}=0.8 \text{ mJy}$ at a redshift of $z = 2.5$. This galaxy is much less luminous and massive than other high- z SMGs. It resembles to similarly luminous dusty starbursts resulting from lower-mass mergers in the local Universe.

In order to link the different population of high-redshift objects, several LBGs at redshift between 2.5 and 4.5 have been targeted at $850 \mu\text{m}$. The Lyman-break technique (Steidel et al. 1996) detects the rest-frame 91.2 nm neutral hydrogen absorption break in the SED of a galaxy as it passes through several broad-band filters. LBGs are the largest sample of spectroscopically confirmed high-redshift galaxies. Observing LBGs in the submillimeter is an important goal, because it would investigate the link, if any, between the two populations. However, the rather low success rate of submillimeter counterpart of LBGs (e.g., Chapman et al. 2000; Webb et al. 2003) argues against a large overlap of the two populations.

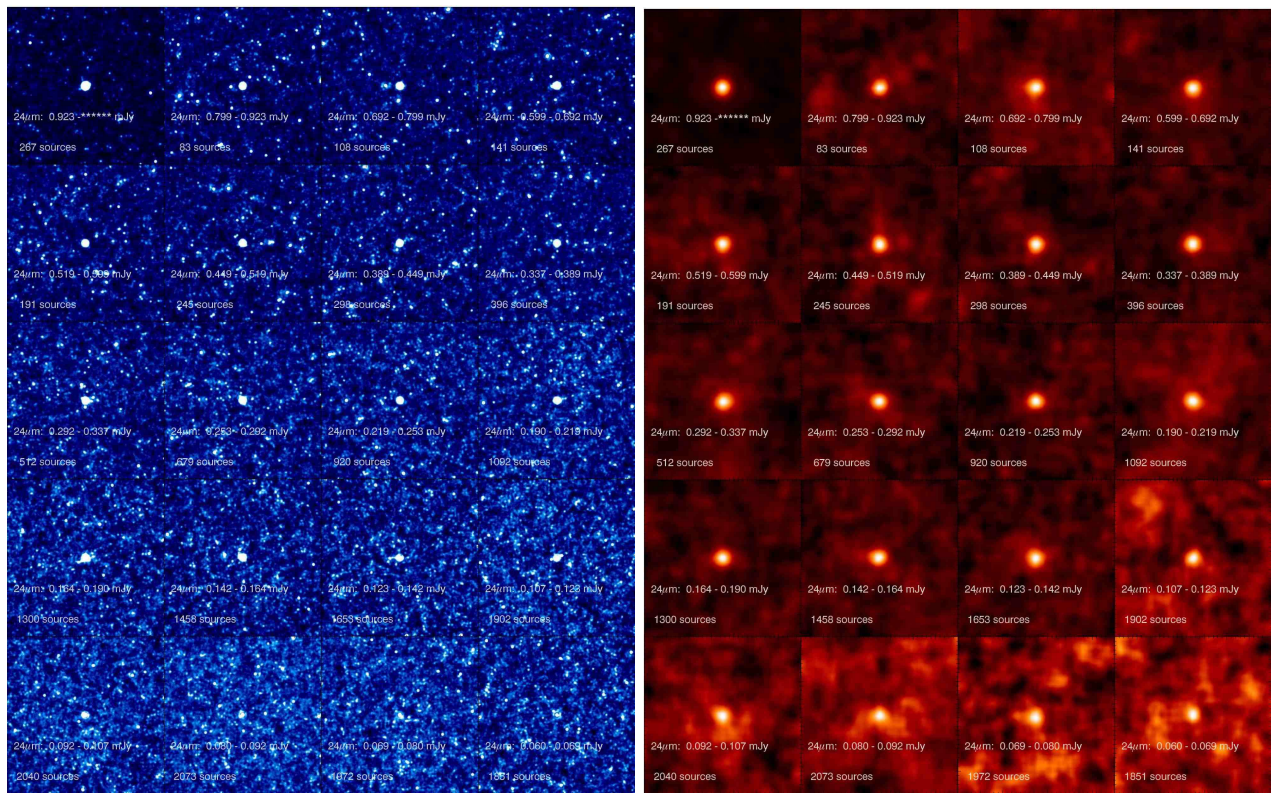


Figure 3: *Left*: Images of stacked *Spitzer* 24 μm sources per bin of 24 μm flux. More than 19000 sources has been used. *Right*: The corresponding stacked images at 160 μm .

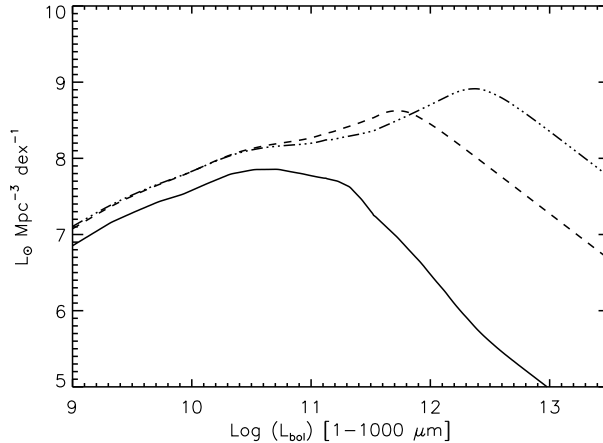


Figure 4: Co-moving evolution of the IR energy output per dex of luminosity ($L \, dN/d\text{Log}L$). The continuous, dashed, dashed-3dotted lines are for $z=0, 0.5$ and 2 respectively. From Lagache et al. (2004).

4.3 SPITZER observations: linking the ISOCAM galaxies and the SMGs

A potential new way to find high- z LIRGs and ULIRGs appeared recently with the launch of the *Spitzer* observatory. Particularly suited to this goal is the $24 \, \mu\text{m}$ channel of the MIPS instrument. Le Floc'h et al. (2004) give the first hint on the $24 \, \mu\text{m}$ selected galaxies. They couple deep $24 \, \mu\text{m}$ observations in the Lockman hole and extended groth strip with optical and near-infrared data to get both identification and redshift (either spectroscopic or photometric). They find a clear class of galaxies with redshift $1 \leq z \leq 2.5$ and with luminosities greater than $\sim 5 \times 10^{11} L_{\odot}$ (see also Lonsdale et al. 2004). These galaxies are rather red and massive with $M > 2 \times 10^{10} M_{\odot}$ (Caputi et al. 2005). Massive star-forming galaxies revealed at $2 \leq z \leq 3$ by the $24 \, \mu\text{m}$ deep surveys are characterized by very high star formation rates – $\text{SFR} \geq 500 M_{\odot} \text{ year}^{-1}$. They are able to construct a mass of $\simeq 10^{11} M_{\odot}$ in a burst lifetime ($\simeq 0.1 \text{ Gyr}$). The $24 \, \mu\text{m}$ galaxy population also comprises sources with intermediate luminosities ($10^{10} \leq L_{\text{IR}} \leq 10^{11} L_{\odot}$) and low to intermediate assembled stellar masses ($10^9 \leq M \leq 10^{11} M_{\odot}$) at $z \leq 0.8$. At low redshifts, however, massive galaxies are also present, but appear to be building their stars quiescently in long timescales (Caputi et al. 2005). At these redshifts, the efficiency of the burst-like mode is limited to low mass $M \leq 10^{10} M_{\odot}$ galaxies. These results support a scenario where star-formation activity is differential with assembled stellar mass and redshift, and proceed very efficiently in massive galaxies (Caputi et al. 2005). In the Lockman Hole, only one galaxy is associated with an X-ray source. This suggests that these galaxies are mostly dominating by star formation, consistent with the findings of Alonso-Herrero et al. (2004) and Caputi et al. (2005). This is also suggested by SEDs that are best fitted by PAH features rather than by strongly rising, AGN-type continua (Elbaz et al. 2005). The selected sources exhibit a rather wide range of MIPS to IRAC flux ratio and optical/near-infrared shapes, suggesting a possibly large diversity in the properties of infrared galaxies at high redshift as noticed by Yan et al. (2004). Based on these first analyzes, together with the interpretation of the number counts (e.g., Lagache et al. 2004), it is clear that the $24 \, \mu\text{m}$ observations will provide the sample to unambiguously characterize the infrared galaxies up to $z \simeq 2.5$.

5 Towards resolving the unresolved CIB

As seen in Sect. 3, despite the great sensitivity and the high S/N ratio achieved by the recent *Spitzer* surveys at 70 and $160 \, \mu\text{m}$, the bulk of the CIB in energy, i.e., the peak at about $150 \, \mu\text{m}$, is not resolved in individual sources (i.e. less than 10% at $160 \, \mu\text{m}$). This is due to the confusion. The dominant contribution at the CIB peak can be inferred from the ISOCAM deep surveys (Sect. 2) but this approach is model-dependent since it uses template SEDs to extrapolate the fluxes measured at $15 \, \mu\text{m}$ to the peak of the CIB. Dole et al. (2005) conduct an original approach. They use a stacking analysis method that takes advantage of the good *Spitzer* $24 \, \mu\text{m}$ channel to fill the gap between the mid-IR and the far-IR surveys. Down to a flux of $60 \, \mu\text{Jy}$, *Spitzer* resolved 79% of the CIB at $24 \, \mu\text{m}$. The process of the stacking analysis is the following. First, the $24 \, \mu\text{m}$ sources are sorted by decreasing fluxes and are put in 20 bins of flux with roughly equal logarithmic width of $\Delta S_{24}/S_{24} \sim 0.15$ (except for the

bin corresponding to the brightest flux). A square image, centered on each 24 μm source is then extracted at both the 24, 70 and 160 μm . The images are finally added to generate a stacked image of sources at the three wavelengths for each 24 μm flux bin (Figure 3). Surprisingly, stacked sources are detected at both 70 and 160 μm up to the faintest 24 μm flux bin. The fraction of resolved CIB (using the Lagache et al. (2004) CIB values) becomes 83% and 66% at 70 and 160 μm , respectively. If new CIB estimates from Dole et al. (2005) are used instead, the fraction of resolved CIB becomes more than 75% at both wavelengths. Dole et al. (2005) thus directly measure that a significant fraction of the far-IR CIB is resolved using the mid-IR galaxies, without any model, nor hypothesis. Deriving the properties of the 24 μm galaxies will thus directly probe the bulk of the CIB.

The stacking analysis also allows for the first time to obtain average SEDs of galaxies from $z=0$ to $z=2$ by stacking the 24 μm galaxies per redshift bin in the Chandra Deep Field South, using the redshifts derived by Caputi et al. (2005). The derived SEDs confirm the strong luminosity evolution from $z=0$ to 2 (as shown in the next section). The observed colors can be qualitatively explained by dusty IR luminous galaxies with an important dust component. Comparison with models is provided in Dole et al. (2005).

6 Cosmic evolution of IR galaxies

Another remarkable property of the IR sources is their extremely high rates of evolution with redshift exceeding those measured for galaxies at other wavelengths and comparable to or larger than the evolution rates observed for quasars. As an example, number counts at 15 μm show a prominent bump peaking at about 0.4 mJy. At the peak of the bump, the counts are one order of magnitude above the non-evolution models. In fact, data require a combination of a $(1+z)^3$ luminosity evolution and $(1+z)^3$ density evolution for the starburst component at redshift lower than 0.9 to fit the strong evolution. Although it has not been possible with ISOCAM to probe in detail the evolution of the infrared luminosity function, *Spitzer* data at 24 μm give for the first time tight constraints up to redshift 1.2 (Le Floc'h et al. 2005; Pérez-González et al. 2005). A strong evolution is noticeable and requires a shift of the characteristic luminosity L^* by a factor $(1+z)^{4.0\pm 0.5}$. Le Floc'h et al. (2005) find that the LIRGs and ULIRGs become the dominant population contributing to the comoving infrared energy density beyond $z \sim 0.5-0.6$ and represent 70% of the star-forming activity at $z \sim 1$. The comoving luminosity density produced by luminous infrared galaxies was more than 10 times larger at $z \sim 1$ than in the local Universe. For comparison, the B-band luminosity density was only three times larger at $z = 1$ than today. Such a large number density of LIRGs in the distant Universe could be caused by episodic and violent star-formation events, superimposed on relatively small levels of star formation activity. These events can be associated to major changes in the galaxy morphologies. The rapid decline of the luminosity density from $z = 1$ is only partially due to the decreasing frequency of major merger events. Bell et al. (2005) showed that the SFR density at $z \sim 0.7$ is dominated by morphologically normal spiral, E/S0 and irregular galaxies ($\geq 70\%$), while clearly interacting galaxies account for $< 30\%$. The dominant driver of the decline is a strong decrease in SFR in morphologically undisturbed galaxies. This could be due, for example, to gas consumption or to the decrease of weak interactions with small satellites that could trigger the star formation through bars and spiral arms.

At still higher redshifts, the infrared luminosity of the sources that dominate the background is larger than $10^{12}L_{\odot}$. This is a population with a very different infrared luminosity function than the local or even the $z = 1$ luminosity function. The global evolution of the IR energy output with redshift is illustrated on Figure 4.

7 Conclusions and Challenges

A number of conclusions are now clear from the analysis of the identified sources in the CIB:

- The comoving energy produced in the past that makes up the CIB at different wavelengths is more uniform than what is suggested by its spectral energy distribution. This is due to the fact that the CIB at long wavelengths ($\lambda \geq 400\mu\text{m}$) is dominated by emission from the peak of the SED of galaxies at high z . More quantitatively, the ISOCAM surveys reveal that about two-thirds of the CIB emission at $\lambda \sim 150 \mu\text{m}$ is generated by LIRGs at $z \sim 0.7$. At 850 μm , more than half of the submillimeter CIB is generated by SMGs. The brightest SMGs ($S_{850} > 3$ mJy, $\sim 30\%$ of the CIB) are ULIRGs at a median redshift of 2.2. The energy density at 150 μm , which is $\sim 20-25$ times larger than the energy density at 850 μm requires a comoving energy production rate at $z = 0.7$ roughly 10 times the energy production rate at $z = 2.2$.
- The evolution exhibited by LIRGs and ULIRGs is much faster than for optically selected galaxies. The ratio of infrared to optical, volume-averaged output of galaxies increases rapidly with increasing redshift.
- Luminosity function evolution is such that the power output is dominated by LIRGs at $z \simeq 0.7$ and ULIRGs at $z \simeq 2.5$.
- The energy output of CIB sources is dominated by starburst activity.

- AGN activity is very common in the most luminous of these galaxies even though this activity does not dominate the energy output. The rate and fraction of the energy produced increase with the luminosity.
- LIRGs at $z \simeq 0.7$ are dominated by interacting massive late-type galaxies. They seem to be starburst phases of already-built massive, late-type field galaxies accreting gas or gas-rich companions forming the disks. We see today a rapid decrease of this activity probably associated with a dry out of the gas reservoir in their vicinity. The larger redshift IR galaxies ($z \simeq 2.5$), which are also more luminous, seem to belong to more massive complex systems involving major merging. These systems could be located in the rare larger amplitude peaks of the large-scale structures leading to massive elliptical galaxies at the center of rich clusters.
- SMGs show rather strong correlations with correlation lengths larger than those of other high redshift sources.
- LIRGs and ULIRGs cannot be identified with any of the distant populations found by rest-frame ultraviolet and optical surveys.

Although these findings are answering the basic questions about the sources that make up the CIB, there are still observational difficulties to be overcome to complete these answers. The SEDs of LIRGs and ULIRGs are quite variable and often not very well constrained in their ratio of far-infrared to mid-infrared or to submillimeter wavelengths. The far-infrared, where most of the energy is radiated, requires cryogenically cooled telescopes. These have small diameters and, hence, poor angular resolution and severe confusion limits for blind surveys. Establishing proper SEDs for the different classes of infrared galaxies detected either in mid-infrared (with ISOCAM at $15 \mu\text{m}$ or MIPS at $24 \mu\text{m}$) or in millimeter-submillimeter surveys is one of the challenges of the coming decade. Making sure that no class of sources that contribute significantly to the CIB at any wavelength has been missed is an other observational challenge. The submillimeter galaxies not found through the radio-selected sources and the question of the warm submillimeter galaxies are also two of those challenges.

References

- [1] Aussel H., Cesarsky C.J., Elbaz D., Starck J.-L. 1999, *A&A* 342, 313
- [2] Alonso-Herrero A., Pérez-gonzález P.G., Rigby J. et al. 2004, *APJS* 154, 155
- [3] Bell E.F., Papovich C., Wolf C., et al. 2005, *ApJ* 625, 23
- [4] Blain A.W., Chapman S.C., Smail I., Ivison R.J. 2004, *ApJ* 611, 725
- [5] Blain A.W., Smail I., Ivison R.J. et al. 2002, *Physics Report* 369, 111
- [6] Caputi K., Dole H., Lagache G. et al., 2005, *ApJ*, in press
- [7] Chanical P., 2003. PhD Thesis. Paris-XI Univ.
- [8] Chapman S.C., Blain A.W, Smail I., Ivison R.J., 2005, *ApJ* 622, 772
- [9] Chapman S.C., Scott D., Steidel C.C., et al., 2000, *MNRAS* 319, 318
- [10] Condon J. J. 1992, *ARAA* 30, 575
- [11] Conselice C.J., Chapman S.C., Windhorst R.A. 2003, *ApJ* 596, 5
- [12] Dole H., Caputi K.I., Lagache G., J.-L. Puget et al., 2005, *A&A* submitted
- [13] Dole H., Le Floc'h E., Pérez-González P.G. et al., 2004, *ApJS* 154, 87
- [14] Dole H., Gispert R., Lagache G. et al. 2001, *A&A* 372, 364
- [15] Elbaz D., Le Floc'h E., Dole H., Marcillac D. 2005, *A&A* 434, 1
- [16] Elbaz D., Césarsky C. 2003, *Science* 300, 270
- [17] Elbaz D., Césarsky C.J., Chanical P. et al. 2002, *A&A* 384, 848
- [18] Fadda D., Elbaz D., Duc P.-A. et al. 2002, *A&A* 361, 827
- [19] Flores H., Hammer F., Elbaz D. et al. 2004, *A&A* 415, 885
- [20] Flores H., Hammer F., Thuan T.X., et al. 1999, *ApJ* 517, 148
- [21] Franceschini A., Berta S., Rigopoulou D. et al. 2003, *A&A* 403, 501
- [22] Genzel R., Baker A.J., Ivison R.J. et al. 2004. Proc. Venice Conf. Multiwavelength Mapping of Galaxy Formation and Evolution. In press

- [23] Genzel R., Baker A.J., Tacconi L. et al. 2003, *A&A* 584, 633
- [24] Genzel R., Lutz D., Sturm E. et al. 1998, *ApJ* 498,579
- [25] Gispert R., Lagache G., Puget J.-L. 2000, *A&A* 360, 1
- [26] Greve T. R., Bertoldi F., Smail I. et al. 2005, *MNRAS* 359, 1165
- [27] Greve T. R., Ivison R. J., Bertoldi, F. et al. 2004, *MNRAS* 354, 779
- [28] Gruppioni C., Lari C., Pozzi F. et al. 2002, *MNRAS* 335, 831
- [29] Hammer F., Flores H., Elbaz D. et al. 2005, *A&A* 430, 115
- [30] Hammer F., Gruel N., Thuan T.X. et al. 2001, *ApJ* 550, 570
- [31] Helou G., Soifer B.T., Rowan-Robinson M. 1985, *ApJ* 298, 7
- [32] Héraudeau P., Oliver S., del Burgo C. et al., 2004, *MNRAS* 354, 924
- [33] Kneib J.-P., Neri R., Smail I., et al. 2005, *A&A* 434, 819
- [34] Kennicutt R.C. 1992, *AJ* 388, 310
- [35] Kennicutt R.C. Jr. 1998, *Ann. Rev. Astron. Astrophys.* 36, 189
- [36] Lagache G., Puget J.-L., Dole H., 2005, *ARAA* 43, 727
- [37] Lagache G., Dole H., Puget J.-L. et al. 2004, *ApJS* 154, 112
- [38] Lagache G., Puget J.-L. 2000, *A&A* 355, 17
- [39] Lari C., Pozzi F., Gruppioni C., et al. 2001 *MNRAS* 325, 1173
- [40] Le Floc'h E., Papovich C., Dole H. et al. 2005, *ApJ*, in press
- [41] Le Floc'h E., Pérez-González P.G., Rieke G.H. 2004, *ApJS* 154, 170
- [42] Liang Y.C., Hammer F., Flores H. et al. 2004, *A&A* 423, 876
- [43] Lonsdale C., Del Carmen Polletta M.C., Surace J. et al., *ApJS* 154, 54
- [44] Lutz D., Spoon H.W.W., Rigopoulou D. et al. 1998, *ApJ* 505, 103
- [45] Mann R.G., Oliver S., Carballo et al. 2002, *MNRAS* 332, 549
- [46] Maloney P.R., Glenn J., Aguirre J.E. et al., 2005, *ApJ*, in press
- [47] Matsuhara H., Kawara K., Sato Y. et al., 2000, *A&A* 361, 407
- [48] Metcalfe L., McBreen B., Kneib J.-P. et al. 2003, *A&A* 407, 791
- [49] Miville-Deschenes M-A., Lagache, G., Puget J-L. 2002, *A&A* 393, 749
- [50] Nakamura O., Fukugita M., Brinkmann J., Schneider D.P. 2004, *AJ* 127, 2511
- [51] Neri R., Genzel R., Ivison R.J. et al. 2003, *ApJ* 597, 113
- [52] Oliver S., Rowan-Robinson M., Alexander D.M. et al. 2000, *MNRAS* 316, 749
- [53] Papovich C., Dole H., Egami E., et al. 2004, *ApJS* 154, 70
- [54] Pérez-González P.G., Rieke G.H., Egami E. et al. 2005, *ApJ* 630, 82
- [55] Sanders D.B., Mirabel F. 1996, *ARAA* 34, 749
- [56] Sato Y., Kawara K., Cowie L.L. et al. 2003, *A&A* 405, 833
- [57] Scott S.E., Fox M.J., Dunlop J.S. et al. 2002, *MNRAS* 331, 817
- [58] Smail I., Chapman S.C., Blain A.W., Ivison R.J., 2004, *ApJ* 616, 71
- [59] Smail I., Ivison R.J., Blain A.W., Kneib J.-P. 2002, *MNRAS* 331, 495
- [60] Soifer B.T., Neugebauer G. 1991, *AJ* 101, 354

- [61] Steidel C.C., Giavalisco M., Pettini M. et al. 1996, *ApJ* 624, L17
- [62] Swinbank A.M., Smail I., Chapman et al. 2005, *ApJ* 617, 64
- [63] Webb T.M., Eales S., Foucaud S. et al., 2003, *ApJ* 582, 6
- [64] Yan L., Helou G. Fadda D. et al. 2004, *ApJS* 154, 60
- [65] Zheng X.Z., Hammer F., Flores H. et al. 2004, *A&A* 421, 847